www.czasopisma.pan.pl PAN www.journals.pan.pl
Chemical and Process Engineering 2019, 40 (1), 87–99
DOI: 10.24425/cpe.2019.126103

Large Eddy Simulation of turbulent flow and heat transfer in a Kenics static mixer

Halina Murasiewicz, Barbara Zakrzewska*

West Pomeranian University of Technology, Szczecin, Institute of Chemical Engineering and Environmental Protection Processes, al. Piastów 42, 71-065 Szczecin, Poland

CFD modelling of momentum and heat transfer using the Large Eddy Simulation (LES) approach has been presented for a Kenics static mixer. The simulations were performed with the commercial code ANSYS Fluent 15 for turbulent flow of three values of Reynolds number, Re = 5 000, 10 000 and 18 000. The numerical modelling began in the RANS model, where standard $k-\varepsilon$ turbulence model and wall functions were used. Then the LES iterations started from the initial velocity and temperature fields obtained in RANS. In LES, the Smagorinsky–Lilly model was used for the sub-grid scale fluctuations along with wall functions for prediction of flow and heat transfer in the near-wall region. The performed numerical study in a Kenics static mixer resulted in highly fluctuating fields of both velocity and temperature. Simulation results were presented and analysed in the form of velocity and temperature contours. In addition, the surface-averaged heat transfer coefficient values for the whole insert length were computed and compared with the literature experimental data. Good compliance of the LES simulation results with the experimental correlation was obtained.

Keywords: heat transfer, turbulent flow, Large Eddy Simulation, CFD, static mixer

1. INTRODUCTION

Static mixers are widely employed in the industry for liquid mixing, as heat and mass transfer promoters or even as chemical reactors in a variety of applications. Several studies were reported in the open literature for Kenics static mixers using both experimental and numerical tools. The papers were dedicated mainly to the geometry optimisation to increase the mixing efficiency by determining the optimal twist angle of the mixing elements for non-creeping flow conditions by employing CFD (Byrde and Sawley, 1999; Hobbs and Muzzio, 1998) using techniques from dynamical systems analysis, including Poincare sections, tracking of fluid tracers. The static mixer geometries of Sulzer SMX mixer were modified and numerically studied by Somana and Madhuranthakam (2017) to improve enhanced mixing performance under laminar flow conditions with an incompressible fluid. Both dispersive mixing and distributive mixing results of modified static mixer geometry showed significant improvement of mixing compared to a standard SMX geometry. The optimisation of Kenics geometry mixer using computational analysis was performed by Szalai and Muzzio (2003), who found the twist angle affects performance at low flow rates ($Re \sim 1$) whereas both the element aspect ratio and the twist angle are shown to be important at high flow rates ($Re \leq 1000$).

There have been numerous studies to investigate pressure drop, e.g. Stec and Synowiec (2017), Kumar et al. (2008) and Song and Han (2005) who derived the new correlations for pressure drop in static mixer based on data collected from either CFD simulation or experiment. For instant, recent researchers Stec

* Corresponding author, e-mail: zakrzewska@zut.edu.pl

and Synowiec (2017) have estimated pressure drop in two static mixers: Kenics and Koflo to establish a model which enable the pressure drop predictions from Eu or Ne number. The method for pressure drops introduced by Kumar et al. (2008) was developed from collected data from measuring the pressure drop per unit element ($\Delta P/\eta$) in three different Kenics and numerical simulations of pressure drop across the mixer. In an earlier study by Song and Han (2005), the pressure drop correlation was described by three dimensionless groups, i.e., the friction factor, Reynolds number, and aspect ratio of a mixing element. A developed correlation can cover an entire range of flow from laminar to turbulent. In all presented above methods a good agreement between estimated and calculated values of pressure drop was found.

Most early studies reported in the literature addressed mixing efficiency. Recently, Meng et al. (2015) estimated mixing performance qualitatively by tracking Poincare sections, and quantitatively by the variation coefficient as a function of axial position. The authors showed that among a variety of tested static mixers, the Kenics static mixer had the best mixing performance whereas right twist-type static mixer (RSM) had two oval-shaped segregated areas which periodically moved clockwise 90 degrees in the cross-sections of adjacent twisted tapes. A similar technique to improve the mixing performance of the Kenics was adopted by Hobbs and Muzzio (1998). The authors also extended their study by using dynamical systems analysis, tracking of fluid tracers, and the development of stretching histories for tracer elements and computing of the variation coefficient. It was found that a substantial increase in mixer efficiency is achieved using elements with less twist than the standard 180 degrees Kenics configuration. Alberini et al. (2014) determined the performance of Kenics static mixers for the blending of two shear-thinning fluid streams with identical or different rheology by using Planar Laser Induced Fluorescence (PLIF). The mixing performance was characterised by comparing conventional mixing measures represented by coefficient of variation and maximum striation area with recent alternative methods such as the areal distribution method. This comparison illustrated the complexity of information-rich PDF images. Previous research of mixing process done by Lang et al. (1995) revealed that the main mixing occurs in the wake of the mixer. It was explained that the vortices generated by the structure of the mixer have been observed to be the main driving force of the mixing of the fluid. Generally, mixing quality was improved significantly by incorporating a static mixer.

Several studies have considered heat transfer in different static mixers (Grace, 1971; Joshi et al., 1995; Lang et al., 1995; Qi et al., 2003) where experiment-based correlations for estimating heat transfer coefficient were presented. A non-dimensional equation for the turbulent flow range was proposed by Grace (1971) and it was in use for several years despite its imperfection. Joshi et al. (1995) proposed a modification to that correlation for wall-fluid heat transfer in the Kenics static mixer in a wide range of Reynolds number. Their correlation was further modified by Myers et al. (1997) based on extensive research performed at Chemineer, Inc. that resulted in proposing Eq. (1) valid for the turbulent flow range.

$$Nu = 0.078 Re^{3/4} Pr^{1/3} \tag{1}$$

Knowledge of the value of heat transfer coefficient in several thermal processes is crucial for the determination of local fluid temperature. It was clearly confirmed that high local temperature differences can detrimentally affect product properties (Qi et al., 2003), especially in modern technologies.

In addition to the experimental approach, an enormous capability of Computational Fluid Dynamics (CFD) codes has been exploited in modern investigations of heat transfer problems. The numerical tool allows for computing local flow and thermal quantities, such as velocity and temperature. However, despite the high potential of CFD a few reports (Chang and Jang, 2012; Lisboa et al., 2010; Meng et al., 2016; Rahmani et al., 2007; Tian and Barigou, 2015; Visser et al.,1999; Zakrzewska and Jaworski, 2006) on numerical studies of heat transfer in static mixers were published in the subject literature. In the relevant publications, heat transfer was modelled only by means of the Reynolds-Averaged Navier–Stokes (RANS) method (Ferziger and Peric, 1996; Hewitt and Vassilicos, 2005), which delivers local and time-averaged values of the simulated variables of momentum and heat transport.

The Large Eddy Simulation (LES) approach, however, is transient and considers the flow of eddies larger than the scale of numerical grid applied. LES is an attractive alternative to RANS approach and is widely used in simulation of chemical engineering problems, e.g. impinging jet reactors (Makowski and Wojtas, 2018), precipitation process (Makowski et al., 2012), combustion (De et al., 2018), stirred tanks (Haringa et al., 2018; Li et al., 2011; Nurtono et al., 2009), gas-cyclone airflow (Dhakal et al., 2014) and swirl flows (Li et al., 2017; Kharoua et al., 2018). LES method allows to follow the evolution of local velocity and temperature and, consequently, the local instantaneous values of heat flux and heat transfer coefficient. An additional purpose of this study was to compare LES results of heat transfer with those obtained in RANS method for the Kenics static mixer.

2. THEORETICAL

Large eddy simulation is a transient formulation that usually provides excellent results for all flow systems. It solves the Navier–Stokes equations for large scale turbulent fluctuations and models only the small-scale fluctuations, smaller in size than a computational cell (Wilcox, 1993). The filtered general variable, ϕ, is defined by

$$\widetilde{\phi_f}(x,t) = \int_D \phi\,(x-r,t)\,G\,(r,x)\,dr \tag{2}$$

where D denotes the fluid domain of integration, G is the typical filter kernel that determines the scale of the resolved eddies and the r coordinate is not distant from x.

The filtering operation can be applied to the original Navier–Stokes and energy equations leading to

$$\frac{\partial \widetilde{u_i}}{\partial x_i} = 0 \tag{3}$$

$$\frac{\partial \widetilde{u_i}}{\partial t} + \frac{\partial\left(\widetilde{u_i}\,\widetilde{u_j}\right)}{\partial x_j} = -\frac{1}{\rho} + \nu\frac{\partial^2 \widetilde{u_i}}{\partial x_j \partial x_j} - \frac{\partial \tau_{ij}}{\partial x_j} \tag{4}$$

$$\frac{\partial\left(\widetilde{p}\,\widetilde{T}\right)}{\partial t} + \frac{\partial}{\partial x_j}\left(\widetilde{\rho}\,\widetilde{u_j}\,\widetilde{T}\right) = \frac{\partial}{\partial x_j}\left(\left(\frac{\mu}{Pr} + \frac{\mu_t}{Pr_t}\right)\frac{\partial \widetilde{T}}{\partial x_j}\right) + \widetilde{\omega}_T \tag{5}$$

where $\widetilde{u}$, $\widetilde{p}$, $\widetilde{T}$, $\widetilde{\rho}$ are filtered velocity, pressure, temperature and density, respectively. Quantity $\widetilde{\omega}_T$ in the last term of Eq. (5) denotes the filtered heat release source term. The subgrid-scale stress, τ_{ij}, is defined by Eq. (6).

$$\tau_{ij} = u_i u_j - \widetilde{u_i}\widetilde{u_j} \tag{6}$$

The subgrid-scale stresses resulting from the filtering operation are unknown and require modelling. The first and still widely used model for τ_{ij} is the Smagorinsky–Lilly model (Hewitt and Vassilicos, 2005), which can be written in the version with the eddy viscosity, μ_t

$$\tau_{ij} - \frac{1}{3}\tau_{kk}\delta_{ij} = -2\mu_t \widetilde{S}_{ij} \tag{7}$$

where $\widetilde{S}_{ij}$ is the strain rate tensor based on the filtered velocity field for the resolved scale (Wilcox, 1993). The isotropic part of the subgrid-scale stresses τ_{kk} is an unknown scalar and should be added to the filtered static pressure term. The eddy viscosity in the Smagorinsky–Lilly model can be expressed analogously to the mixing-length model

$$\mu_t = (C_s\Delta)^2\left|\widetilde{S}\right| \qquad \text{where} \quad \left|\widetilde{S}\right| = \sqrt{2\widetilde{S}_{ij}\widetilde{S}_{ij}} \tag{8}$$

The value of C_S varies depending on the flow type and various applications have been done with $0.1 < C_S < 0.24$ (Wilcox, 1993). However, numerical investigations revealed that the best results for

a wide range of flows were obtained for the C_S value of around 0.1 (Lesieur, 1997). In practical applications of LES it is usually assumed that the width of the grid filter, $\overline{\Delta}$, should be locally close to the magnitude of the lateral Taylor microscale of turbulence, λ_g. For the fully developed turbulent flow, the relationship of Eq. (9) can be assumed.

$$\overline{\Delta} \cong \lambda_g \cong \sqrt{10\frac{\mu k}{\rho \varepsilon}} \tag{9}$$

Thus, the local size of the applied grid of 1.5 M cells was compared also in this study with the local Taylor microscale of turbulence. For the considered cases, the average values of the turbulence kinetic energy, k, and its rate of dissipation, ε, were calculated from the RANS simulation results. The mean values of k, ε, the average cell size and Taylor microscale, λ_g, are collected in Table 1 for the 3 levels of turbulent Reynolds number.

The average length of computational cells for the applied mesh of 1.5 million (1.5 M) cells was 1.52×10^{-3} m, which is very close to the Taylor microscale shown in Table 1.

Table 1. Values of k, ε and λ_g for three *Re* levels

Reynolds number, *Re*	k, m^2s^{-2}	ε, m^2s^{-3}	λ_g, m
5 000	0.0008	0.003	1.63×10^{-3}
10 000	0.0035	0.021	1.29×10^{-3}
18 000	0.0119	0.131	0.96×10^{-3}

Another important requirement in LES simulation is the application of time increments corresponding to the critical Courant number of 1/20, by analogy to direct simulations (Pope, 2000). Therefore, the time step in the iterations, Δt should be chosen so that

$$\Delta t \cong \frac{\lambda_g}{20\sqrt{k}} \tag{10}$$

Turbulent Prandtl number, $Pr_t = \dfrac{\mu_t}{C_p \lambda_t}$, appears in the energy transport equation, Eq. (5), and its value is close to 1.0 for the fully developed flow (Launder and Spalding, 1974). However, near walls it assumes slightly smaller values than 1.0 and direct numerical simulations (DNS) of turbulent momentum and energy transport revealed that the value of turbulent Prandtl number is variable (So and Sommer, 1996). In our numerical investigations, a constant value of $Pr_t = 0.85$ was assumed.

The filtered total heat flux is defined by

$$\widetilde{q} = -C_p \left(\frac{\mu}{Pr} + \frac{\mu_t}{Pr_t} \right) \frac{\partial \widetilde{T}}{\partial x_j} \tag{11}$$

In general, the modelling of turbulent heat transfer is crucially linked to the way we model the boundary layer. In the LES approach, the model type depends on the size of computational cells within the boundary layer and on the filter applied (Pope, 2000). If both the filter and the numerical grid are sufficiently fine in the layer to resolve 80% of the flow energy, then the momentum balance equation is directly solved by the LES method. However, if the filter and grid are too coarse to correctly represent the near-wall motions, then their influence is derived from a boundary layer model. Even at high Reynolds number, the near-wall motion is not explicitly computed in the viscous wall region and the boundary conditions similar to the standard wall functions are used in the modelling (Launder and Spalding, 1974).

3. MODELLING METHODOLOGY

A CFD numerical study was performed for a Kenics static mixer with six inserts. The simulations were based on the LES approach for a single phase of physical properties for water. Kenics inserts, twisted by 180° alternatively clock-wise and counter clock-wise, were placed in the pipe (Fig. 1). The insert diameter was equal to 0.0736 m with the aspect ratio (length to diameter of insert) equivalent to 1.5 and the total length of the Kenics mixer was L = 1.152 m. The detailed dimensions of the Kenics static mixer elements are presented in Table 2. The numerical mesh was created with the help of a specialised pre-processor Gambit 2.0.4 with the total number of control volumes (cells) formed by the grid of about 1.5 million (1.5 M). The simulations were carried out for turbulent flow of the three different Reynolds number values, Re = 5 000; 10 000 and 18 000 using the commercial code Fluent 15.

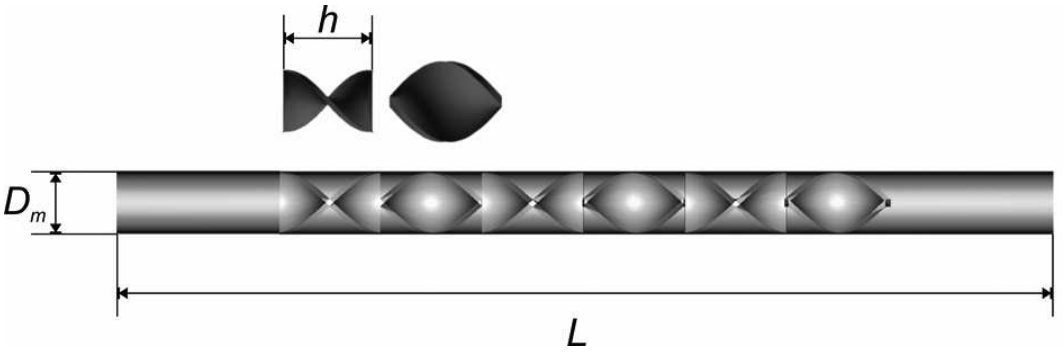

Fig. 1. Kenics mixer geometry

Table 2. Basic dimensions of the static mixer elements

Dimension	Kenics static mixer
Pipe diameter, D_m, m	0.0736
Pipe length L, m	1.152
Number of mixing elements	6
Mixing element length, h, m	0.113
Inlet length, m	0.135

The numerical modelling began in the RANS mode for the flow in the static mixer with heat transfer (steady-state, time-averaged process), where standard $k-\varepsilon$ turbulence model and wall functions were used. Then the LES iterations started from the initial velocity and temperature fields obtained in RANS. The large eddy simulations used the Smagorinsky–Lilly model (Pope, 2000) and wall functions along with the energy equation for determining transient fields of flow and temperature. The single time step was $\delta t = 10^{-3}$ s and the total simulation time was Δt = 1.0 s. Within each of the 1000 time steps done, 50 SIMPLEC iterations were performed to couple velocities and pressure fields. The second order upwind difference scheme was selected for all quantities (continuity, momentum, and turbulence) to stabilise simulation, accompanied by the standard under-relaxation factors for the RANS simulation. For LES, the second order scheme was used for pressure. For momentum, the Bounded Central Differencing scheme was preferred because it produces low numerical diffusion. The iterations were continued until the normalised sum of residuals reached the level of 10^{-7}.

The boundary conditions for heat transfer were defined constant for the mixing elements, inlet part of the pipe wall and the liquid temperature at the inlet to the mixer at the level of 293 K. The temperature of the

remaining part of the pipe wall was set to 363 K and this was called the heating wall (Fig. 2). The value of the mean axial velocity at the inlet to the pipe and fluid properties were also set to yield the required Reynolds number.

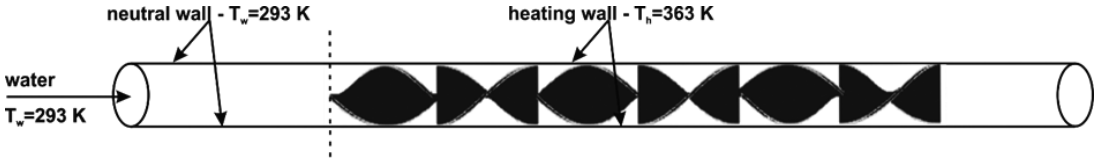

Fig. 2. Thermal boundary conditions

4. RESULTS

This study of the flow field and heat transfer was done for three different Reynolds numbers of 5 000; 10 000 and 18 000. The numerical grid of 1.5 M size was used in the two methods: *unsteady* LES and *steady-state* RANS. Turbulent flows are characterised by fluctuating velocity fields, which mix transported quantities of mass, momentum, and energy and, in turn, cause the transported quantities to fluctuate as well. The simulation results for the three levels of Reynolds number allowed to visualise the instantaneous fields of velocity and temperature inside the Kenics mixer. An example of the contour map of the axial liquid velocity for the cross section in the middle of the 5th insert is shown in Fig. 3a. Detailed analysis of the velocity and temperature fields was focused on the fifth insert downstream since the LDA measurements (Adamiak and Jaworski, 2001) proved that turbulence in that mixer area can be regarded as fully developed. The LES results were analysed for the final simulation time of 1.0 s for each of the three Reynolds numbers of 5 000; 10 000; 18 000, respectively. The analysis of momentum transfer is presented here only for the most important, axial velocity component. However, the two other velocity components were also stored for further examination. The simulation data were visualised in the form of maps of the axial velocity component. The average axial velocity in the middle of the 5th insert for the three different *Re* were about 0.074 m/s, 0.146 m/s, 0.264 m/s, respectively. The local LES values of the axial velocity component in the mid-cross section of the 5th insert were time-averaged and compared with the corresponding steady-state RANS values and a satisfactory agreement was always found.

Fig. 3a presents the axial velocity contours at the middle of the fifth mixing element for three Reynolds numbers, obtained from LES simulations and for time step Δt = 1.0 s. The instantaneous, local axial velocity was varying in the range from −0.20 to 0.59 m/s. The contours show fluctuations of the velocity and illustrate the location of the maximum and minimum local axial velocities. In addition, the maps reveal local turbulent eddies of large scale.

This confirms the flow is inhomogeneous and highly swirling, which is characteristic for turbulent flows. The simulated vortex structures strongly fluctuate in time and space inside the mixers. A favourable comparison of the simulated mean pressure drop with the available literature data suggests the LES modelling properly reflects the turbulent flow conditions.

Distributions of fluid temperature were presented in an analogous way to the velocity maps, also for the three *Re* levels. An example of the contour map of the fluid temperature obtained in the LES for the middle cross-section of the fifth mixing element is shown in Fig. 3b. The temperature extent for the simulation time of 1.0 s covers the range from 293 to 320 K. The fluid temperature, and the fluid velocity fluctuated in the insert space with the maximum values close to the mixer wall and gradually decreased in the direction of the insert wall. That observation was valid for the three *Re* values. Local temperature was recorded during the large eddy simulations and this allowed to derive its average in the period from 0 to 1 s. The averages were 305.47 K, 302.03 K and 301.11 K respectively for *Re* = 5 000; 10 000 and 18 000. In the

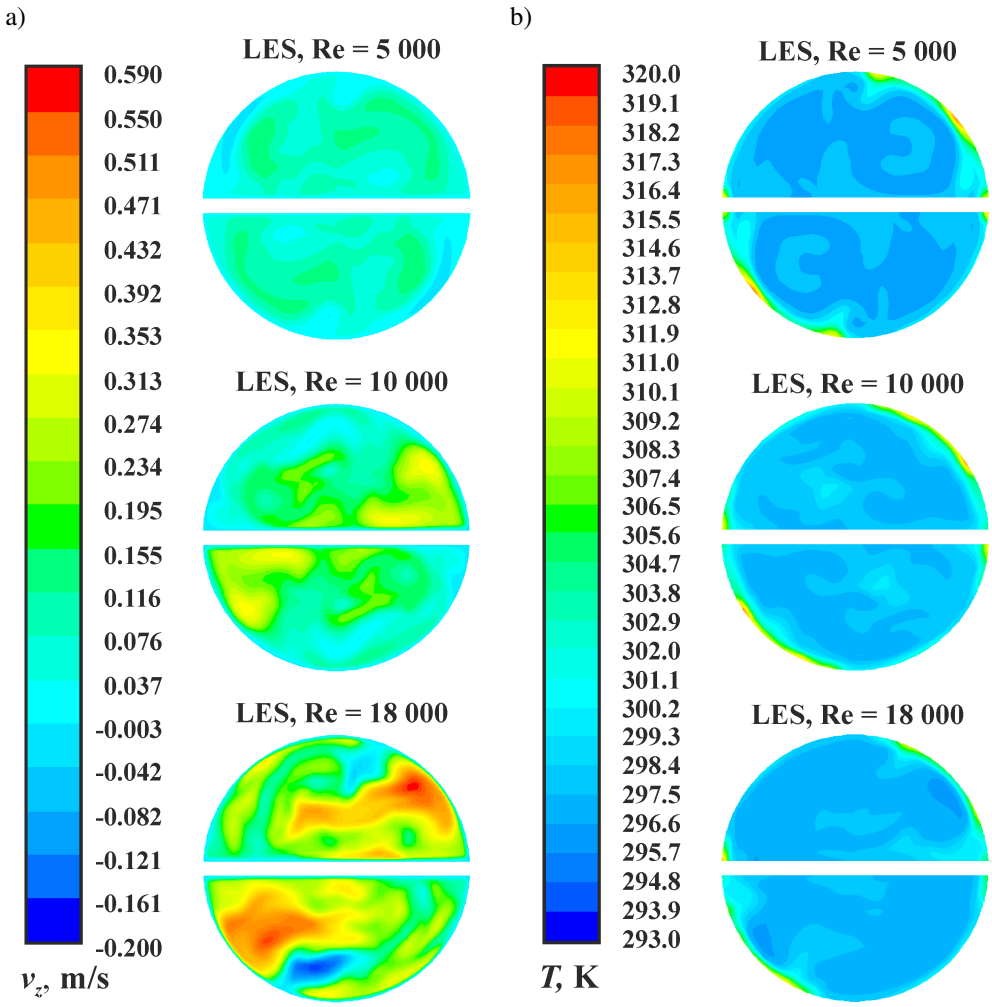

Fig. 3. Contours of: a) axial velocity, b) water temperature at the middle of the fifth mixing element; Re = 5 000; 10 000; 18 000; 1.5 M grid size; Δt = 1.0 s

RANS mode, however, the average fluid temperature was slightly lower being 305.41 K, 301.95 K and 301.07 K for Re = 5 000; 10 000 and 18 000, respectively.

For the sake of efficient, visual presentation of the fluid temperature distribution inside the insert area, a map of the temperature contours was prepared for Re of 18 000 (Fig. 4).

Although fluid temperature varies with different intensity, it tends to have the highest values at the mixer heating wall. The areas of different fluid temperature reflect the inhomogeneous structure of the turbulent fluid flow. It was also noted that the regions of high and low fluid temperature match corresponding regions of fluid velocity and the shape of the regions are similar too. That analogy was observed for all three Re values of the turbulent flow.

The accomplished LES modelling enabled us to examine the time evolution of the temperature field from the beginning of the transient simulations to the stage of nearly pseudo-steady state. However, analysis of the temperature data provided evidence that the simulation results stored for the simulated period of flow time of 1.0 s did not demonstrate a sufficiently long pseudo-steady state since the temperature evolution still exhibited its slow increase. This condition means the simulations may still require further continuation.

In addition, the predicted values of the local heat transfer coefficient were computed for each time step. The surface-averaged heat transfer coefficient values, h_{ave}, for the whole insert length and for the three levels of Reynolds number were then compared with the literature experimental data (Eq. (1)). The data obtained

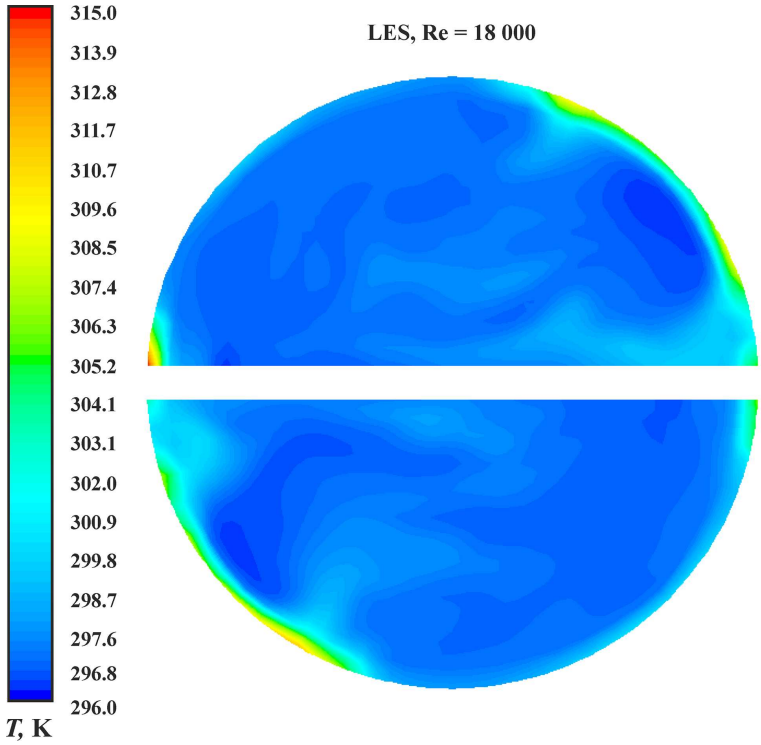

Fig. 4. Contours of water temperature in the middle of the fifth mixing element; Re = 18 000; 1.5 M grid size; Δt = 1.0 s

in that way were collected in Table 3. In general, the predicted values of the heat transfer coefficient for the Kenics static mixer were close to those obtained experimentally.

Table 3. Comparison of the averaged heat transfer coefficient values, h_{ave}, for the RANS and LES modelling

Methods	Reynolds number	Heat transfer coefficient, $h_{ave,\,CFD}$	Experimental heat transfer coefficient, $h_{ave,\,exp}$ (Eq. (1))	Relative difference between $h_{ave,\,CFD}$ and $h_{ave,\,exp}$ [%]
RANS	5 000	963.6	1106.5	12.9
	10 000	1380.0	1926.4	28.4
	18 000	2256.0	3083.0	26.8
LES	5 000	1037.1	1106.5	6.3
	10 000	1431.7	1926.4	25.7
	18 000	1998.0	3083.0	35.2

Nevertheless, departures of the CFD simulated values $h_{ave,\,CFD}$, from the experimental, $h_{ave,\,exp}$ (Eq.1) obtained in the large eddy simulations were smaller for the turbulent flow of Re = 5 000 and 10 000 than for 18 000. The differences were respectively close to 6.3 % and 25.7%. On the other hand, in the RANS method, the differences were slightly higher and close to 12.9% and 28.4%, respectively for Re = 5 000 and 10 000. An opposite situation was found for Reynolds number of 18 000, where lower deviations between $h_{ave,\,CFD}$ and $h_{ave,\,exp}$ were obtained for the RANS modelling and they were 26.8 % for RANS and as much as 35.2% for LES. It is anticipated that the most probable cause of the high differences between the modelling and experiment was due to the use of the hydrodynamic and thermal wall functions in predicting the turbulent energy transport in the boundary layer of the Kenics static mixer by the two

modelling methods. The wall functions used in Fluent require the dimensionless values of the distance from the centre of the computational cell adjacent to the wall, y^+, to be higher than 30. The numerical grid used in the simulations was very dense and the resultant average values of the y^+ value were 7.50, 12 and 18 for Re = 5 000; 10 000 and 18 000, respectively, for RANS and LES as well. It means that for such low y^+ values another type of the boundary layer model should be rather applied, which would account for the laminar sub-layer. In the case of the Fluent code that criterion is fulfilled by the enhanced wall treatment and it will be used in the next stage of the heat transfer simulations in the Kenics static mixer. That treatment can be used both in the RANS and LES approaches. It is anticipated that the use of those wall functions should lower the differences between the averaged values of the heat transfer coefficient derived from the simulations and calculated from the experimental correlation, Eq. (1).

Contours of the local values of the heat transfer coefficient, h, at the wall of the fifth and sixth mixing Kenics element and the three applied Re levels were presented in Fig. 5. The contours shown there were computed from the data generated in the LES computations for the total time of 1.0 s. Those contours indicate that the highest local values of the heat transfer coefficient were obtained for Re = 18 000. The distributions of the coefficient values for the three levels of Re reveal a certain level of inhomogeneity. The areas of the minimum and maximum values of h appear close to each other, which suggest high fluctuations in time and space. Application of the large eddy modelling approach for simulating heat transfer at turbulent fluid flow in the static mixer gave the opportunity to examine the nature of fluctuation of the local heat transfer coefficient in the selected region of the mixer wall.

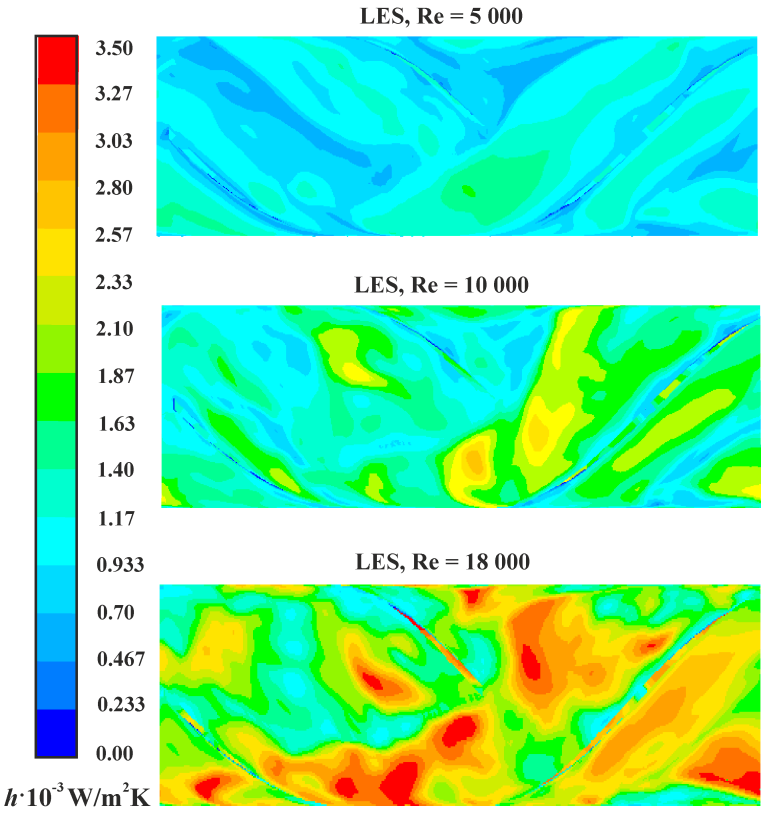

Fig. 5. Contours of the local heat transfer coefficient, h, at the heating wall surrounding the fifth and sixth mixing elements obtained for water and 1.5 M grid size, Δt = 1.0 s, LES approach

Analogous contours of the local heat transfer coefficient were prepared also for the 5th and 6th Kenics elements for the RANS modelling data (Fig. 6). In a comparable manner to the LES results, the maximum values of the heat transfer coefficient were obtained for Re = 18 000. However, it was noticed that the h

values derived from the RANS modelling are slightly higher than those from LES. The maximum value appearing in Fig. 6 is close to $3.5 \cdot 10^3$ W/m^{2}K. It was also found that the distribution of the coefficient h, obtained for the RANS method and the three analysed Re levels have a more uniform character. It most likely follows from the time-average mode in RANS for the local values resulting in smoothing of the flow fluctuations that are present in turbulent flows. Therefore, the applied LES method allowed to better trail the character of the heat transfer coefficient distribution, which is very valuable in heat transfer analyses.

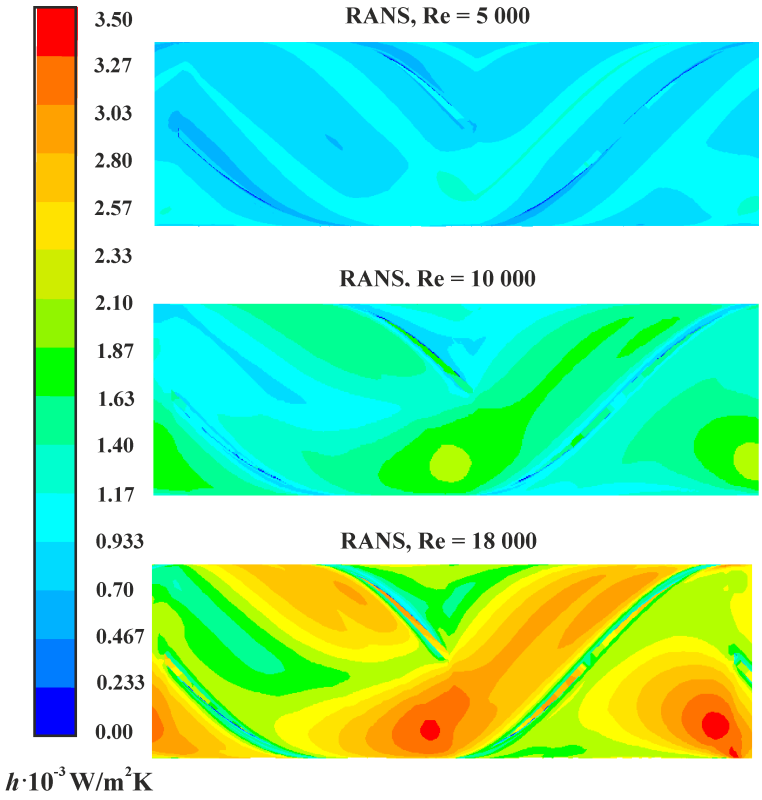

Fig. 6. Contours of the local heat transfer coefficient, h, at the heating wall surrounding the fifth and sixth mixing elements obtained for water and 1.5 M grid size, RANS approach

5. CONCLUSIONS

The performed numerical study of the turbulent heat transfer in a Kenics static mixer with the use of large eddy simulations resulted in highly fluctuating fields of both velocity and temperature. Instantaneous and time-averaged characteristics of the flow and heat transfer were computed. Differences in the averaged values of heat transfer coefficient from CFD and experiment were found. It was also concluded that the LES technique can be successfully applied to simulate turbulent heat transfer in the Kenics static mixer.

The following specific conclusions were drawn based on the simulation results:

- Analysis of the turbulent flow field by means of large eddy simulations allowed to reconstruct the fluid flow structure, both its mean and eddy components appearing in the flow.
- It was observed that the evolution of velocity and temperature in the region of the fifth insert occurred in an equivalent way for Re = 5 000 resulting in the matching of the regions of their maximum and minimum values.
- The minimum difference between the averaged values of the heat transfer coefficient predicted by LES and those from experiments was obtained at the level of 6.3% and 25.7% for Re = 5 000 and 10 000, respectively.

- For Re = 18 000 and the RANS simulations, a lower discrepancy between the $h_{ave,\,\mathrm{CFD}}$ and $h_{ave,\,\mathrm{exp}}$ values was found for those in the LES approach. The corresponding values were 26.8 % and 35.2%, respectively for RANS and LES.
- One of the major sources of the disagreement between the predictions and experiments for the heat transfer coefficient for the two simulation methods can be attributed to the use of the standard wall functions for resolving the boundary layer.
- Large eddy simulations can be applied to the modelling of heat transfer in the static mixer. However, to further diminish the discrepancy between experiments and simulations a more precise model for the boundary layer should be applied.
- Results for the reported total LES simulation time of 1.0 second did not fully prove the pseudo-steady state of heat transfer in the Kenics mixer was already achieved and perhaps the simulations should be further prolonged.
- The LES approach allows to numerically study the dynamics of the flow and temperature fields and to reconstruct the flow structure in the mixer.

SYMBOLS

C_p	heat capacity, J/(kgK)
C_s	Smagorinsky constant
h, h_{ave}	local and averaged heat transfer, W/m^{2}K
k	kinetic energy of turbulence, m^2/s^2
Nu	Nusselt number
p	pressure, Pa
Pr, Pr_t	molecular and turbulent Prandtl number
Re	Reynolds number
$\widetilde{S}_{ij}$	filtered strain rate tensor, 1/s
t	time, s
T	temperature, K
u	velocity, m/s
y^+	non-dimensional distance from wall

Greek symbols

Δ	filter width, m
Δt	time step, s
ε	energy dissipation rate, m^2/s^3
λ_t	turbulent thermal conductivity, W/(mK)
μ, μ_t	molecular and turbulent dynamic viscosity, kg/(ms)
ρ	density, kg/m^3

Superscripts

$\sim$	filtered quantities

Subscripts

ave	averaged value
CFD	CFD simulation
exp	experimental
i , j	Cartesian coordinates

REFERENCES

Adamiak I., Jaworski Z., 2001. Experimental studies of non-Newtonian liquid flow in the Kenics static mixer. *Chem. Process Eng.*, 22, 3B, 157–180 (in Polish).

Alberini F., Simmons M.J.H., Ingram A., Stitt E.H., 2014. Assessment of different methods of analysis to characterise the mixing of shear-thinning fluids in a Kenics KM static mixer using PLIF. *Chem. Eng. Sci.*, 112, 152–169. DOI: 10.1016/j.ces.2014.03.022.

Byrde O., Sawley, M. 1999. Optimization of a Kenics static mixer for non-creeping flow conditions. *Chem. Eng. J.*, 72, 163–169. DOI: 10.1016/S1385-8947(98)00145-4.

Chang K.-T., Jang J.-H., 2012. Heat transfer characteristics with insertion of tri-helical static mixers in pipes. *Progress Comput. Fluid Dyn., Int. J. (PCFD)*, 12(4). DOI: 10.1504/PCFD.2012.048251.

De S., Agarwal A.K., Chaudhuri S., Sen S., 2018. *Modeling and simulation of turbulent combustion*. Springer, Singapore. DOI: 10.1007/978-981-10-7410-3.

Dhakal T.P., Walters D.K., Strasser W., 2014. Numerical study of gas-cyclone airflow: an investigation of turbulence modelling approaches. *Int. J. Comput. Fluid Dyn.*, 28, 1–15. DOI: 10.1080/10618562.2013.878800.

Ferziger J.H., Peric M., 1996. *Computational methods for fluid dynamics*. Springer. Berlin.

Grace C.D., 1971. Static mixing and heat transfer. *Chem. Proc. Eng.*, 52, 57–59.

Haringa C., Vandewijer R., Mudde R.F., 2018. Inter-compartment interaction in multi-impeller mixing. Part II. Experiments, sliding mesh and large Eddy simulations. *Chem. Eng. Res. Des.*, 136, 886–899. DOI: 10.1016/j.cherd.2018.06.007.

Hewitt G., Vassilicos Ch., 2005. *Prediction of turbulent flows*. Cambridge University Press, Cambridge.

Hobbs D.M., Muzzio F.J., 1998. Optimization of a static mixer using dynamical system techniques. *Chem. Eng. Sci*., 53, 3199–321. DOI: 10.1016/S0009-2509(98)00115-8.

Joshi P., Nigam K.D.P., Bruce Nauman E., 1995. The Kenics static mixer: New data and proposed correlations. *Chem. Eng. J.*, 59, 265–271. DOI: 10.1016/0923-0467(94)02948-2.

Kharoua N., Khezzar L., Alshehhi M., 2018. The interaction of confined swirling flow with a conical bluff body: Numerical simulation. *Chem. Eng. Res. Des.*, 136, 207–218. DOI: 10.1016/j.cherd.2018.04.034.

Kumar V., Shirke V., Nigam K.D.P., 2008. Performance of Kenics static mixer over a wide range of Reynolds number. *Chem. Eng. J.*, 139, 284–295. DOI: 10.1016/j.cej.2007.07.101.

Lang E., Drtina P., Streiff F., Fleischli M., 1995. Numerical simulation of the fluid flow and the mixing process in a static mixer. *Int. J. Heat Mass Transfer*, 38, 2239–2250. DOI: 10.1016/0017-9310(94)00351-U.

Launder B.E., Spalding D.B., 1974. The numerical computation of turbulent flows. *Comp. Meth. Applied Mech. Eng.*, 3, 269–289. DOI: 10.1016/0045-7825(74)90029-2.

Lesieur H., 1997. *Turbulence in fluids, stochastic and numerical modelling*. Kluwer Academic Publishers, Dordrecht.

Li G., Miles N.J., Wu T., Hall P., 2017. Large eddy simulation and Reynolds-averaged Navier–Stokes based modelling of geometrically induced swirl flows applied for the better understanding of Clean-In-Place procedures. *Food Bioprod. Process.*, 104, 77–93. DOI: 10.1016/j.fbp.2017.05.001.

Li Z., Bao Y., Gao Z., 2011. PIV experiments and large eddy simulations of single-loop flow fields in Rushton turbine stirred tanks. *Chem. Eng. Sci.*, 66, 1219–1231. DOI: 10.1016/j.ces.2010.12.024.

Lisboa P.F., Fernandes J., Simões P.C., Mota J.P.B., Saatdjian E., 2010. Computational-fluid-dynamics study of a Kenics static mixer as a heat exchanger for supercritical carbon dioxide. *J. Supercrit. Fluids*, 55, 107–115. DOI: 10.1016/j.supflu.2010.08.005.

Makowski Ł., Orciuch W., Bałdyga J., 2012. Large eddy simulations of mixing effects on the course of precipitation process. *Chem. Eng. Sci.*, 77, 85–94. DOI: 10.1016/j.ces.2011.12.020.

Makowski Ł., Wojtas K., 2018. Large Eddy Simulations on selected problems in chemical engineering. In: Ochowiak M., Woziwodzki S., Doligalski M., Mitkowski P. (Eds), *Practical aspects of chemical engineering. Lecture notes on multidisciplinary industrial engineering*. Springer, Cham. 243–262. DOI: 10.1007/978-3-319-73978-6_17.

Meng H., Zhu G., Yu Y., Wang Z., Wu J., 2015. Chaotic mixing characteristics in static mixers with different axial twisted-tape inserts. *Can. J. Chem. Eng.*, 93,1849–1859. DOI: 10.1002/cjce.22268

Meng H., Zhu G., Yu Y., Wang Z., Wu J., 2016. The effect of symmetrical perforated holes on the turbulent heat transfer in the static mixer with modified Kenics segments. *Int. J. Heat Mass Transfer*, 99, 647–659. DOI: 10.1016/j.ijheatmasstransfer.2016.03.110.

Myers K.J., Bakker A., Ryan D., 1997. Avoid agitation by selecting static mixers. *Chem. Eng. Progress*, 93(6), 28–38.

Nurtono T., Setyawan H., Altway A., Winardi S., 2009, Macro-instability characteristic in agitated tank based on flow visualization experiment and large eddy simulation. *Chem. Eng. Res. Des.*, 87, 923–942. DOI: 10.1016/j.cherd.2009.01.011.

Pope S., 2000. *Turbulent flows*. Cambridge University Press, Cambridge.

Qi Y., Kawaguchi Y., Christensen R. N., Zakin J. L., 2003. Enhancing heat transfer ability of drag reducing surfactant solutions with static mixers and honeycombs. *Int. J. Heat Mass Transfer*, 46, 5161–5173. DOI: 10.1016/ S0017-9310(03)00221-7.

Rahmani R. K., Ayasoufi A., Keith T.G., 2007. A numerical study of the global performance of two static mixers. *J. Fluids Eng.*, 129, 338–349. DOI: 10.1115/IMECE2005-79189.

So R.M., Sommer T.P., 1996. An explicit algebraic heat-flux model for the temperature field. *Int. J. Heat Mass Transfer*, 39, 455–465. DOI: 10.1016/0017-9310(95)00157-5.

Somana S.S., Madhuranthakam C.M.R., 2017. Effects of internal geometry modi?cations on the dispersive and distributive mixing in static mixers. *Chem. Eng. Process. Process Intensif.*, 122, 31–43. DOI: 10.1016/j.cep.2017.10.001.

Song S., Han H., 2005. A general correlation for pressure drop in a Kenics static mixer. *Chem. Eng. Sci.*, 60, 5696–5704. DOI: 10.1016/j.ces.2005.04.084.

Stec M., Synowiec P.M., 2017. Study of fluid dynamic conditions in the selected static mixers. Part I – Research of pressure drop. *Can. J. Chem. Eng.*, 95, 2156–2167. DOI: 10.1002/cjce.22929.

Szalai E. S., Muzzio F., 2003. Fundamental approach to the design and optimization of static mixers. *AIChE J.,* 49, 2687–2699. DOI: 10.1002/aic.690491103.

Tian S., Barigou M., 2015. An improved vibration technique for enhancing temperature uniformity and heat transfer in viscous fluid flow. *Chem. Eng. Sci.*, 123, 609–619. DOI: 10.1016/j.ces.2014.11.029.

Visser J.E., Rozendal P.F., Hoogstraten H.W., Beenackers A.A.C.M.,1999. Three-dimensional numerical simulation of flow and heat transfer in the Sulzer SMX static mixer. *Chem. Eng. Sci.*, 54, 2491–2500. DOI: 10.1016/ S0009-2509(98)00536-3.

Wilcox D.C., 1993. *Turbulence modelling for CFD*. DCW Indus. Inc., La Cañada, California.

Zakrzewska B., Jaworski Z., 2006. Modelling of heat transfer in static mixers. *Chem. Process Eng.*, 27, 547–557.

Received 28 August 2018
Received in revised form 15 January 2019
Accepted 28 January 2019